THE JOURNAL OF BIOLOGICAL CHEMISTRY Vol. 277, No. 36, Issue of September 6, pp. 33300–33310, 2002
Printed in U.S.A.

MLN64 Mediates Mobilization of Lysosomal Cholesterol to Steroidogenic Mitochondria*[S]

Received for publication, January 2, 2002, and in revised form, June 14, 2002
Published, JBC Papers in Press, June 17, 2002, DOI 10.1074/jbc.M200003200

Mei Zhang‡§, Pei Liu§¶, Nancy K. Dwyer‡, Lane K. Christenson¶, Toshio Fujimoto¶, Federico Martinez¶‖, Marcy Comly‡, John A. Hanover, E. Joan Blanchette-Mackie‡ ‡‡, and Jerome F. Strauss III¶§§**

*From the ‡Lipid Cell Biology Section and **Cell Biochemistry Section, Laboratory of Cell Biochemistry and Biology, NIDDK, National Institutes of Health, Bethesda, Maryland 20892 and ¶Center for Research on Reproduction and Women's Health, University of Pennsylvania Medical Center, Philadelphia, Pennsylvania 19104*

This study demonstrates that the steroidogenic acute regulatory protein-related lipid transfer (START) domain-containing protein, MLN64, participates in intracellular cholesterol trafficking. Analysis of the intracellular itinerary of MLN64 and MLN64 mutants tagged with green fluorescent protein showed that the N-terminal transmembrane domains mediate endocytosis of MLN64 from the plasma membrane to late endocytic compartments. MLN64 constitutively traffics via dynamic NPC1-containing late endosomal tubules in normal cells; this dynamic movement was inhibited in cholesterol-loaded cells, and MLN64 is trapped at the periphery of cholesterol-laden lysosomes. The MLN64 START domain stimulated free cholesterol transfer from donor to acceptor mitochondrial membranes and enhanced steroidogenesis by placental mitochondria. Expression of a truncated form of MLN64 (ΔSTART-MLN64), which contains N-terminal transmembrane domains but lacks the START domain, caused free cholesterol accumulation in lysosomes and inhibited late endocytic dynamics. The ΔSTART-MLN64 dominant negative protein was located at the surface of the cholesterol-laden lysosomes. This dominant negative mutant suppressed steroidogenesis in COS cells expressing the mitochondrial cholesterol side chain cleavage system. We conclude that MLN64 participates in mobilization and utilization of lysosomal cholesterol by virtue of the START domain's role in cholesterol transport.

Cells obtain cholesterol by either low density lipoprotein (LDL)[1] receptor-mediated endocytosis of LDL or *de novo* synthesis in the endoplasmic reticulum (1). Endocytosed cholesterol moves to the late endocytic compartment and subsequently modulates homeostatic responses via SREBP-SCAP located in the endoplasmic reticulum and Golgi (2). Mutations in *NPC1* and *NPC2* cause Niemann-Pick type C (NPC) disease, characterized by a phenotype of excessive cholesterol accumulation in lysosomes (3, 4). Although *NPC1* and *NPC2* are required for egress of lysosomal cholesterol, the mechanism by which cholesterol is removed from the late endocytic pathway, a dynamic tubular network that communicates with lysosomes, is not known.

The mysteries of lysosomal cholesterol transport began to be unraveled when the gene responsible for the majority of cases of NPC disease, *NPC1*, was cloned (3). NPC1, a protein with a sterol-sensing domain, spans the surface membrane of the late endosomal compartment, and cellular uptake of low density lipoproteins promotes enrichment of NPC1 in late endosomes (5–7). The sterol-sensing domain was shown to be critical for cholesterol transfer, confirmed by the findings based on site-directed mutagenesis and protein trafficking analysis of NPC1 protein (5–7). NPC1 was recently suggested to be a permease that may be involved in material transfer across the endosomal/lysosomal limiting membrane (8). The critical role of another protein, HE1, in clearing cholesterol out of lysosomes was established when it was discovered that the *HE1* gene is mutated in the second and less frequent form of Niemann-Pick type C disease and is, therefore, the *NPC2* gene. *HE1* encodes a soluble cholesterol-binding protein (4, 9).

Recently, MLN64, a protein that contains a C-terminal StAR-related lipid transfer (START) domain was found to reside in late endosomes and lysosomes (10–12). The N terminus of MLN64 consists of a 6-amino acid leader sequence and four anchoring transmembrane domains (10). The START domain binds cholesterol and can stimulate sterol transfer between membranes (10, 13, 14). The topology of MLN64 in late endosomal membranes predicts that the START domain projects into the cytoplasm, where it is positioned to effect cholesterol transfer to opposing membranes (12). The location of a START domain protein in late endocytic pathway with NPC1 and HE1 suggests that MLN64 is a component of the machinery that facilitates cholesterol egress from lysosomes. To investigate this possibility, we elucidated the trafficking, in living cells, of

* This work was supported by National Institutes of Health Grant HD06274 (to J. F. S.) and a grant from the Ara Parseghian Medical Research Foundation. The costs of publication of this article were defrayed in part by the payment of page charges. This article must therefore be hereby marked "*advertisement*" in accordance with 18 U.S.C. Section 1734 solely to indicate this fact.

[S] The on-line version of this article (available at http://www.jbc.org) contains eight QuickTime movies.

§ Both authors contributed equally to this work.

‖ A Visiting Scholar from the Department of Biochemistry, Universidad Nacional Autonoma de Mexico, supported by Fogarty International Center Grant D43-TW-00671.

‡‡ To whom correspondence may be addressed: Lipid Cell Biology Section, Bldg. 8, Rm. 427, NIDDK, National Institutes of Health, 8 Center Dr., MSC 0851, Bethesda, MD 20892. Tel.: 301-496-2050; Fax: 301-402-0723; E-mail: joanbm@bdg8.niddk.nih.gov.

§§ To whom correspondence may be addressed: 1354 BRB II/III, University of Pennsylvania Medical Center, 421 Curie Blvd., Philadelphia, PA 19104. Tel.: 215-898-0147; Fax: 215-573-5408; E-mail: jfs3@mail.med.upenn.edu.

[1] The abbreviations used are: LDL, low density lipoprotein; NPC, Niemann-Pick type C; NPC1, Niemann-Pick type C1 protein; StAR, steroidogenic acute regulatory protein; START, StAR-related lipid transfer; CHO, Chinese hamster ovary; GFP, green fluorescent protein; CFP, cyan fluorescent protein; YFP, yellow fluorescent protein; RFP, red fluorescent protein; CCD, charge-coupled device; MOPS, 4-morpholinepropanesulfonic acid; WT, wild type.

This paper is available on line at http://www.jbc.org

wild type and mutant MLN64 proteins fused with green fluorescent protein (GFP). We found that a truncated MLN64 without the START domain (ΔSTART-MLN64) is a dominant negative mutant. The dominant negative action of this mutant caused extensive cholesterol accumulation in CHO cells and COS-7 cells accompanied by inhibition of late endosomal tubular trafficking, similar to the NPC phenotype that is caused by loss of function of NPC1 and NPC2 (3, 4, 7). This dominant negative mutant also inhibited steroidogenesis in cells. An *in vitro* assay provided evidence that the START domain mediates cholesterol transfer between membranes and stimulates mitochondrial metabolism of cholesterol into steroid hormones. These findings strongly suggest that MLN64 plays a role in the maintenance of intracellular cholesterol homeostasis.

EXPERIMENTAL PROCEDURES

Construction of Expression Plasmids for MLN64-GFP, MLN64-CFP, ΔSTART-MLN64-GFP, START-MLN64-GFP, and NPC1-YFP—The human MLN64 cDNA has been previously described (10). MLN64 cDNA encoding either full-length or specific domains of the MLN64 protein were fused to the green fluorescent protein (pEGFP-N2; CLONTECH Laboratories Inc., Palo Alto, CA). All of the cDNAs used in making these fluorescent fusion proteins were generated by PCR using either *Pfu* or *Taq*DNA polymerases. The PCR primer pair used for the MLN64-GFP (forward, ATTAGAATTCATGAGCAAGCTGCCCAGGGAG; reverse, TAATGTCGACTGATGCGCTGTCGCAGGTGAAAG) spanned the cDNA encoding for amino acids 1–436 of the human MLN64 protein. The MLN64-CFP was constructed by replacing the GFP of MLN64-GFP with CFP from pECFP-N2 (CLONTECH). The START domain for MLN64 (amino acids 216–445) was also PCR-amplified and fused to the GFP vector. A shared forward PCR primer (ATTAGAATTCCGCCACCATGGGGTCTGACAATGAATCAGATG) for generation of the GFP construct was used with the START-MLN64-GFP-specific reverse primer (TAATGTCGACTGATGCGCTGTCGCAGGTGAAAG). The ΔSTART-MLN64-GFP fusion protein was generated by restriction digestion with *Xmn*I and *Sma*I and gel isolation of the vector DNA plus cDNA encoding amino acids 1–225 followed by ligation of the blunt ends to form the ΔSTART-MLN64-GFP construct. All constructs were sequenced and compared with the human MLN64 cDNA sequence (GenBank™ accession numbers NM 006438 and NM 006445, respectively). The human StAR-RFP fusion protein was constructed with the RFP tag pDsRed1 N1 vector (CLONTECH) on the C terminus of the full-length coding sequence of StAR. The human NPC1-YFP fusion protein was constructed by inserting NPC1 together with the six-histidine linker from vector pNES6 (7) into pEYFP-N1 (CLONTECH) in frame with the N terminus of YFP. The function of NPC1-YFP was confirmed by analyzing cholesterol clearance in CT60 cells using filipin staining (data not shown). The F2 expression plasmid, which encodes a fusion protein consisting of the P450 side chain cleavage enzyme and its electron donor (adrenodoxin and adrenodoxin reductase) partners (15), was generously provided by Dr. Walter L. Miller (University of California, San Francisco). An expression plasmid for murine type II 3β-hydroxysteroid dehydrogenase was kindly provided by Dr. Anita Payne (Stanford University). Plasmids for transfection were prepared using the Qiagen Maxiprep system.

Cell Culture and Transfection—For assays of steroidogenic activity (16) of the GFP fusion constructs, COS-1 were cultured in Dulbecco's minimal essential medium supplemented with 10% fetal calf serum and 50 μg of gentamycin/ml in 5% CO_2, 95% air at 37 °C for cell propagation and plating. These cells were obtained from the American Type Culture Collection (Manassas, VA). COS-1 cells were plated at 30,000 cells/well in 12-well plates on day 0. On day 1, cells were transfected with FuGENE6 (Roche Molecular Biochemicals) plus plasmid DNA in the presence of serum as described in the manufacturer's protocol. Cells were co-transfected overnight with 250 ng of each of the 3β-hydroxysteroid dehydrogenase and F2 expression plasmids and 500 ng of the GFP fusion vectors. On day 2, medium was changed to Dulbecco's minimal essential medium containing 10% fetal calf serum. Some cultures were incubated with (22*R*)-hydroxycholesterol, a soluble steroidogenic substrate, to assess maximal hormone production (10). After 24 h, medium was collected and frozen at −20 °C until steroid analysis (see "Progesterone Assays"), and cells were harvested for protein determinations.

To examine utilization of LDL-derived cholesterol, human LDL was reconstituted with [^{3}H]cholesterol linoleate by the method of Krieger *et al.* (17). COS-1 cells transfected with the various MLN64 constructs and the steroidogenic enzymes as described above were cultured in medium supplemented with 10% lipoprotein-deficient serum and 50 μg of protein/ml (70 μg of cholesterol/ml)-reconstituted LDL (0.85×10^5 dpm/μg of cholesterol). The culture medium was collected 40 h later, and radiolabeled progesterone was isolated as described by Soto *et al.* (18).

Wild type CHO cells, CT60 CHO cells, and COS-7 cells were used for microscopic analysis. Cells were maintained in Ham's F-12 medium (CHO cell lines) or McCoy's medium (COS-7 cells and fibroblasts) containing 10% fetal bovine serum (HyClone, Logan, UT). Before transfection, cells were seeded in LabTek chambered coverslips and grown for 20 h to achieve ~60% confluence before transfection. All of the cell lines were transfected using FuGENE6 according to the manufacturer's instructions with some modification. For each chamber of the two-chamber coverslips, cells were incubated with mixtures containing 1 μg of DNA and 4 μl of FuGENE6 reagent in 400 μl of Ham's F-12 medium for 5 h followed by culture in 10% fetal bovine serum-containing Ham's F-12 medium. Transfected cells were either imaged as live cells at different times of expression of the transfected cDNAs or as fixed cells (in 3% paraformaldehyde for 30 min) stained with 50 mg/ml filipin (Polysciences, Warrington, PA) to examine lysosomal cholesterol content (7). For live cell imaging, cells were grown on chambered coverslips (LabTek), and temperature was maintained using a combination of a heating stage and an Objective Heater System (Bioptechs, Butler, PA).

Progesterone Assays—Medium samples from transfected cells were assayed using progesterone Coat-A-Count tubes and reagents (Diagonistic Products Corp., Los Angeles, CA) as described by the manufacturer. Statistical tests were performed using the JMP 3.1.5 computer program (SAS Institute Inc., Cary, NC). One-way analysis of variance was used to analyze the effect of the expression plasmids on steroidogenic activity. Tukey-Kramer mean separation tests were performed for comparison between the means with $p < 0.05$ taken as the level of significance.

Immunoblotting—Western blotting was used to confirm expression of the GFP fusion proteins and the coupling of GFP to the MLN64 sequences. The rabbit MLN64 antiserum was generated against recombinant MLN64 START domain as a His_6 fusion protein (see below). An antiserum to GFP was obtained from Roche Molecular Biochemicals. Western blotting was carried out as described by Watari *et al.* (10).

Production of Recombinant MLN64 START Domain and Assay of Biological Activity—The human MLN64 START domain (amino acid residues 216–445) was expressed in *Escherichia coli* as a His_6 tag protein with the tag on the START domain C terminus using a pET vector, and the protein was purified using previously described methods (13, 14). The recombinant protein was used to generate rabbit anti-MLN64 antibodies. It was also tested for sterol transfer activity as described by Kallen *et al.* (14) in an assay that measures transfer of [^{14}C]cholesterol from unilamellar egg phosphatidylcholine to heat-treated liver mitochondria acceptor membranes. Preliminary studies demonstrated that steroidogenic mitochondria from bovine corpus luteum or human placenta also served as equivalently effective acceptor membranes for START domain-stimulated sterol transfer. Transfer of [^{3}H]triolein incorporated into the liposomes was measured to correct for liposome fusion or trapping. The sterol transfer activity of recombinant MLN64 START domain was compared with that of sterol carrier protein 2.

Preparations enriched in syncytiotrophoblast mitochondria were prepared from human term placenta as described by Martinez *et al.* (19). The mitochondria were incubated in 120 mM KCl, 10 mM MOPS, 0.5 EGTA, 10 mM isocitrate, 0.1% bovine serum albumin, 0.4 μg of aprotinin/0.1 ml, 1 μM leupeptin, pH 7.4, with or without recombinant proteins (19). Reactions were terminated by the addition of methanol, and progesterone was assayed as described above. Progesterone present at zero time was subtracted from values obtained at various time points of incubation.

Pharmacological Perturbations—Wild type CHO cells were treated with progesterone (10 μg/ml) plus LDL (100 μg/ml) to induce cholesterol accumulation in lysosomes (7, 20). To assess the effect of microtubule disruption on MLN64-GFP trafficking, cells were cultured in 10% fetal bovine serum-containing medium with 10 μM nocodazole (Sigma) for up to 2 h at 37 °C.

Labeling Endocytic Pathway in Living Cells—Late endocytic compartments (late endosomes and lysosomes) were labeled by incubating cells with fluorescent dextran (5, 7). Cells were cultured at 37 °C, in medium containing 1 mg/ml rhodamine-dextran (dextran, tetramethylrhodamine, M_r 70,000, lysine-fixable; Molecular Probes, Inc., Eugene, OR) for 1 h of uptake plus 1 h of chase (2 h of uptake/chase time), or 17 h

of uptake plus 1 h of chase (18 h of uptake/chase time) before live cell imaging.

Immunostaining—Cells were fixed with 3% paraformaldehyde in phosphate-buffered saline for 30 min to 1 h, washed in phosphate-buffered saline, and immunostained with mouse monoclonal anti-C-terminal MLN64 antibody (10) at 1:500 dilution and the secondary antibody, Alexa Fluor 568-conjugated goat anti-mouse IgG (Molecular Probes) at 1:100 dilution.

Confocal Microscopy and Time Lapse Imaging—Confocal images were collected using an LSM410 confocal microscope system equipped with a krypton-argon Omnichrome laser with excitation wavelengths of 488 and 568 nm for GFP and rhodamine (and Alexa Fluor 568), respectively (Carl Zeiss Inc., Thornwood, NY), and an argon ion laser (Coherent, Santa Clara, CA) with an excitation wavelength of 351 nm for filipin. Emissions were collected with a C-apochromat 63 × 1.2 NA water immersion objective (Zeiss) using a 514–540-nm band pass filter for GFP, a 590-nm long pass filter for rhodamine and DsRed RFP, and a 400–435-nm band pass filter for filipin.

Time lapse images were captured using a cooled CCD camera (CoolSNAP HQ Monochrome; Photometrics, Tucson, AZ), with a Sony Interline high quantum efficiency chip and custom macros provided by BioVision Technologies. The camera was attached to an Axiovert 35 inverted microscope (Zeiss) with a plan Apochromat 100 × 1.4 NA oil immersion objective (Zeiss) or a C-apochromat 63 × 1.2 NA water immersion objective (Zeiss). The excitation was from a 100-watt Hg-Arc lamp (Atto Instruments Inc., Rockville, MD) with standard fluorescein and rhodamine optics for GFP and RFP, respectively. For CFP and YFP, exciters 395–425 and 460–480 nm, dichroic 505DCXR, and emitter 505–555 nm were used. For dual color time lapse imaging of CFP/YFP or GFP/RFP in co-transfected cells, cells were imaged at 20 °C to slow late endosomal tubular movement. Either CFP and YFP or GFP and RFP were excited and collected sequentially with a time interval of 0 s to minimize time lag during switching channels. IPLab software system (Scanalytics, Fairfax, VA) and custom scripts provided by BioVision Technologies were used for image capture, processing, animation, and export to QuickTime movies. Adobe Photoshop 5.0 was also used for image processing (Adobe Systems Inc., San Jose, CA).

RESULTS

Characterization of the Expression of Wild Type and Mutant MLN64-GFP Fusion Proteins—The fusion protein constructs, MLN64-GFP, START-MLN64-GFP, and ΔSTART-MLN64-GFP, used in this study are shown schematically in Fig. 1. Western blotting using anti-GFP or anti-MLN64 antibodies demonstrated that GFP is attached to MLN64 (Fig. 1, *A* and *B*), ΔSTART-MLN64 (Fig. 1*C*), and START-MLN64 (Fig. 1, *D* and *E*). We detected a low molecular weight band in cells transfected with MLN64-GFP with anti-GFP antibody (Fig. 1*B*). This band was not found either in cells at early times after transfection with MLN64-GFP (15 h) when the MLN64-GFP was found mainly on the plasma membrane (see below) or in cells transfected with ΔSTART-MLN64-GFP or START-MLN64-GFP. This GFP-positive protein is probably derived from post-translational proteolysis in which GFP is cleaved from the MLN64 protein. We do not yet have an antibody recognizing the MLN64 N terminus. However, in extracts of cells transfected with ΔSTART-MLN64 the anti-GFP antibody detected a single protein of the expected molecular weight of the mutant-GFP fusion protein. Similarly, analysis of cells transfected with the START-MLN64-GFP expression plasmid revealed a single MLN64- and GFP-positive protein of the anticipated molecular weight of the fusion protein. We obtained similar results when the plasmids were introduced into either COS or CHO cells.

Although MLN64 has been localized to late endosomes (12), the path that it takes to reach this destination has not been identified. To study the biosynthetic pathway of MLN64, we followed the expression of MLN64-GFP in living CT60 CHO cells that have mutations in the *NPC1* gene and thus display a cholesterol trafficking defect (Fig. 2). 12–17 h after transfection, we found that MLN64-GFP was mainly associated with the plasma membrane (Fig. 2*A*). Very little MLN64-GFP fluorescence was present in cholesterol-laden lysosomes that were labeled by rhodamine dextran uptaken by the cells for 17 h before transfection (data not shown) (7). 72 h after transfection, MLN64-GFP was mainly present as ring-shaped structures (Fig. 2*B*) recognized by immunostaining with anti-C-terminal MLN64 antibody (Fig. 2*C*). Filipin staining confirmed that MLN64-GFP was at the periphery of cholesterol-loaded lysosomes (data not shown). These observations confirm that MLN64-GFP travels first to the plasma membrane before being targeted to the late endocytic compartment. In wild type CHO cells, MLN64-GFP followed an identical biosynthetic pathway to the plasma membrane (data not shown) and then to the late endocytic pathway (see below), as in CT60 cells.

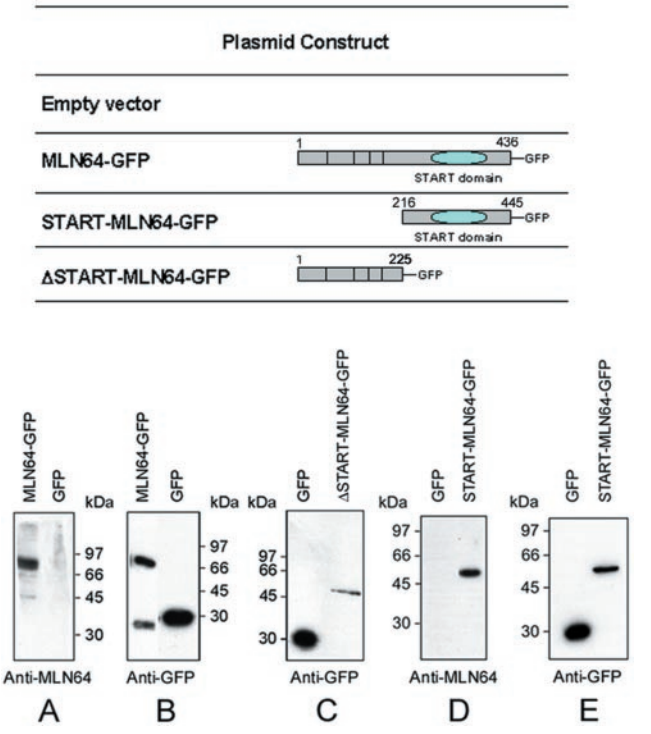

FIG. 1. **Western blot analysis of GFP fusion protein constructs.** A schematic representation of each of the fusion protein constructs is shown. Extracts of COS cells transfected with the indicated plasmids were prepared 48 h after transfection and subjected to Western blotting using an anti-human MLN64 START domain antibody or anti-GFP antibody (five blots, *A–E*). *Blots A* and *B* show that MLN64-GFP was detected by using anti-MLN64 or anti-GFP antibodies at the predicted molecular mass of 78 kDa (51 + 27 kDa). GFP was detected by anti-GFP antibody at 27 kDa (*B*) and was not detected by anti-MLN64 antibody (*A*). A small band was detected by anti-GFP antibody from cells transfected with MLN64-GFP (*B*; discussed under "Results"). *Blot C* shows that ΔSTART-MLN64-GFP was detected as a single band at a molecular mass of 54 kDa (27 + 27 kDa) by using anti-GFP antibody. *Blots D* and *E* show that START-MLN64-GFP was detected by using anti-MLN64 and anti-GFP antibodies as a single band of 55 kDa (28 + 27 kDa).

The ΔSTART-MLN64-GFP followed a biosynthetic trafficking pathway similar to that of wild-type MLN64, first to the plasma membrane (Fig. 2*D*) and then to the cholesterol-laden lysosomes (Fig. 2*E*), showing that ΔSTART-MLN64-GFP contains the essential signals for plasma membrane localization and lysosomal targeting similar to newly synthesized MLN64. ΔSTART-MLN64-GFP is not recognized by the anti-C-terminal MLN64 antibody (Fig. 2*F*). START-MLN64-GFP, the mutant lacking the N-terminal domains, was present only in a cytoplasmic and nuclear pattern 16–72 h after transfection, further substantiating the role of the N-terminal domain in directing MLN64 to the plasma membrane and then to the late endocytic compartment (see below). ΔSTART-MLN64-GFP (Fig. 2*G*) and

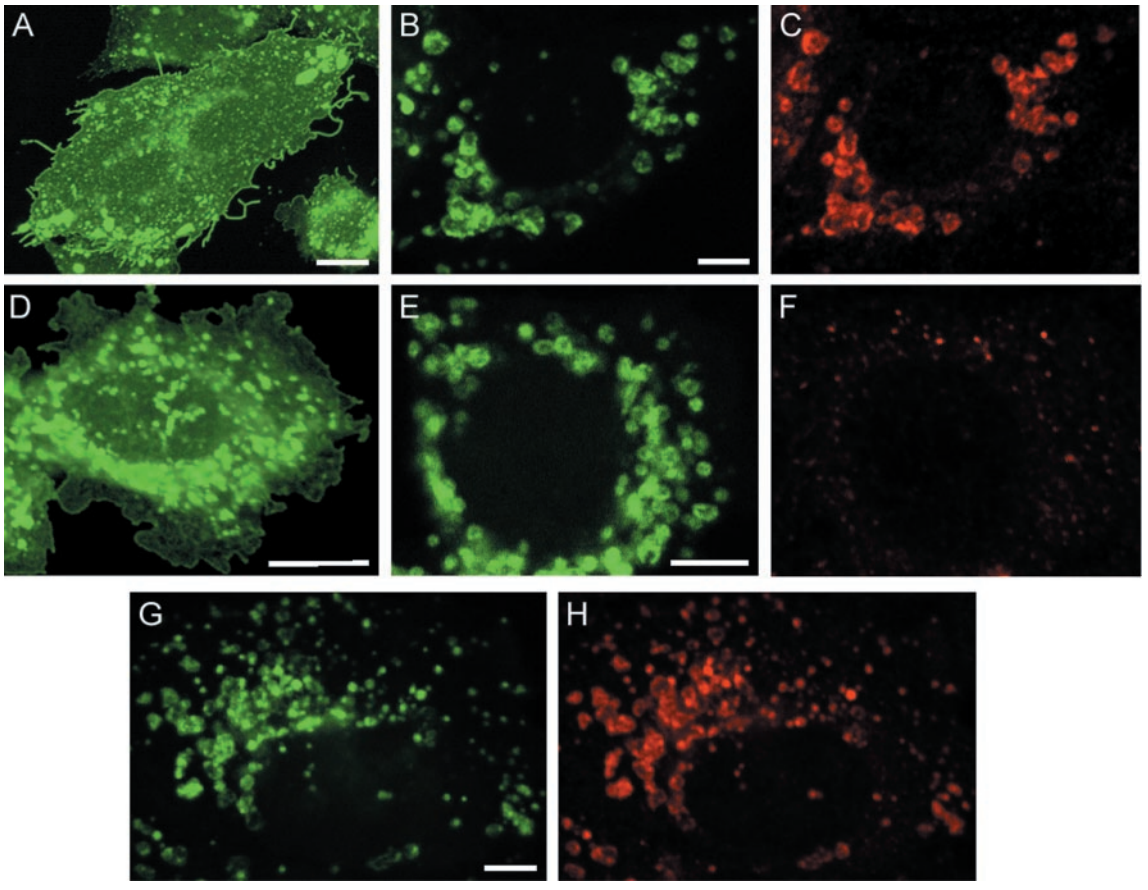

FIG. 2. **Similar biosynthetic trafficking of MLN64-GFP and ΔSTART-MLN64-GFP in cholesterol-laden CT60 CHO cells.** Shown are CT60 CHO cells (NPC1 mutant) transfected with MLN64-GFP (*A–C*), ΔSTART-MLN64-GFP (*D–F*), or co-transfected with nontagged MLN64 and ΔSTART-MLN64-GFP (*G–H*). 24 h after transfection, MLN64-GFP was found mainly on the plasma membrane and in associated small vesicles (*green* in *A*). 72 h after transfection with MLN64-GFP (*green* in *B*) CT60 cells were stained with anti-MLN64 monoclonal antibody (*red* in *C*). MLN64-GFP and anti-MLN64 co-localize at the surface of cholesterol-laden lysosomes. The GFP-tagged truncated MLN64 (ΔSTART-MLN64-GFP), containing the N-terminal transmembrane domains of MLN64, was also delivered to the plasma membrane (*green* in *D*) at an early time of transfection (16 h after transfection) and internalized from plasma membrane to cholesterol-laden lysosomes (*green* in *E*) at later times of transfection (72 h). ΔSTART-MLN64-GFP is not stained by the anti-MLN64 antibody (*F*), because it lacks the antigenic START domain. The ΔSTART-MLN64-GFP (*green* in *G*) was found to be co-localized with wild type MLN64 (*red* in *H*; stained with anti-MLN64 antibody) at the surface of cholesterol-laden lysosomes 72 h after transfection. These results show that wild type MLN64 and ΔSTART-MLN64-GFP mutant traffic together in the same cellular organelles. All images are confocal. *Bars* for *A* and *D*, 10 μm; *bars* for *B*, *C*, and *E–H*, 5 μm.

MLN64 (Fig. 2*H*) co-localized at the periphery of cholesterol-loaded lysosomes in CT60 cells co-transfected with ΔSTART-MLN64-GFP and nontagged MLN64. The nontagged MLN64 was identified with the anti-C-terminal MLN64 antibody. The fact that ΔSTART-MLN64 and MLN64 follow an identical biosynthetic trafficking pathway and locate together at the surface of cholesterol-containing compartments provides morphological evidence that the mutant MLN64 interferes with the role of endogenous MLN64 in cholesterol mobilization from lysosomes (see "Results").

MLN64 Constitutively Traffics within the Cholesterol-regulated, Dynamic Late Endosomal Tubulovesicular Network—We used WT CHO cells transiently transfected with MLN64-GFP or stably expressing MLN64-GFP. MLN64-GFP was found in late endosomal tubulovesicular compartments that constitutively traffic in a microtubule-dependent manner (supplemental movies 1 and 2). The dynamic late endosomal tubular movement is inhibited by nocodazole (10 μM), which disrupts the microtubular network. Similar to previous findings on NPC1 trafficking (7), within 8 min after nocodazole treatment, the MLN64-GFP-containing endosomal compartments ceased to bud tubules and gathered in the perinuclear region, showing little movement (data not shown).

Analysis of living cells cotransfected with MLN64-CFP (Fig. 3, *A* and *C*) and NPC1-YFP (Fig. 3, *B* and *D*) confirmed that MLN64 colocalizes and traffics in the same dynamic late endosomal tubules as NPC1 (supplemental movie 3). As we predicted, MLN64 containing late endosomal trafficking is sensitive to its cholesterol content. In WT CHO cells transfected with MLN64-GFP and exposed to LDL and progesterone, MLN64-GFP (Fig. 3*E*) was localized at the periphery of lysosomes (Fig. 3*F*), similar to the location of NPC1 (7, 21). Late endosomal tubules were rarely observed in the progesterone plus LDL-treated cells. Late endosomal tubular trafficking was also not observed in cholesterol-laden NPC2 and CT60 cells transfected with MLN64-GFP (data not shown). These data show that both MLN64 and NPC1 traffic in late endosomal tubules and the tubular mobility is inhibited when cells accumulate endocytosed cholesterol.

We examined the potential for the endosomal tubules to come into close proximity with mitochondria by imaging cells co-transfected with MLN64-GFP and StAR-RFP, which labels the mitochondrial matrix (supplemental movie 4). We noted parallel alignment of late endosomal tubules with mitochondria in living cells. The late endosomal tubules extending from vesicles increase the surface area of the late endocytic compartment and provide more sites for potential close association with mitochondria, where cholesterol transfer could be effected. Because MLN64-GFP was not anticipated to enter into the mitochondrial matrix, close approximation, but not overlap of the

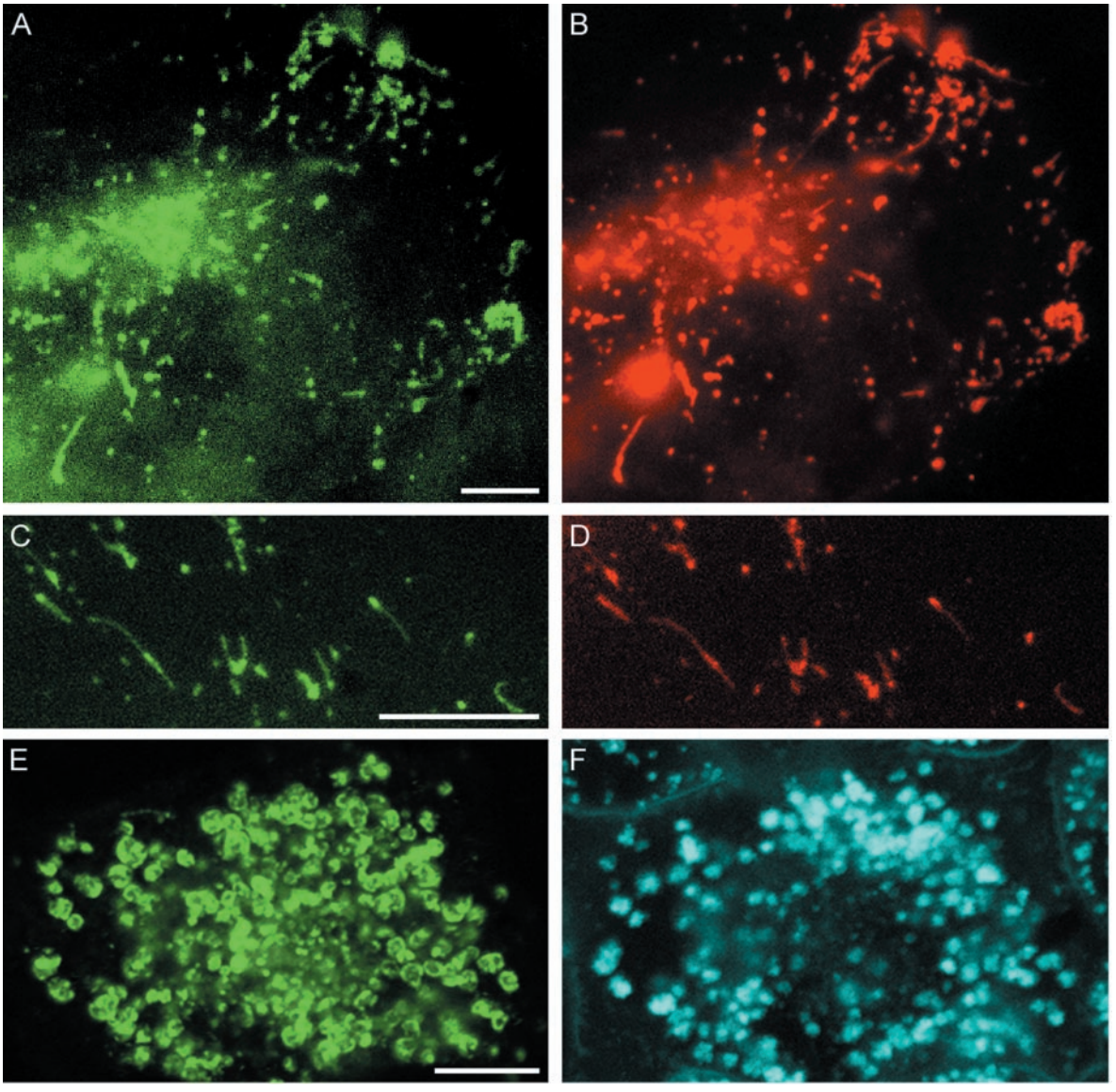

FIG. 3. **MLN64 traffics with NPC1 in late endosomal tubules that are sensitive to cholesterol.** Wild type CHO cells were co-transfected with MLN64-CFP and NPC1-YPF for 96 h (*A* and *B*) or 48 h (*C* and *D*). MLN64-CFP is present in tubulovesicular structures (*green* in *A* and *C*) that also contain NPC1-YFP (*red* in *B* and *D*). Time lapse movies that show late endosomal tubular trafficking of MLN64-GFP transiently expressed in wild type CHO cells at 37 °C (movie 1) or stably expressed in wild type CHO cells at 20 °C (movie 2) and trafficking of both MLN64-CFP and NPC1-YPF in late endosomal tubules (movie 3) at 20 °C are available as supplementary data. Wild type CHO cells were transfected with MLN64-GFP for 48 h and incubated with LDL in the presence of progesterone for 24 h to cause cholesterol loading of lysosomes (*E* and *F*). Cells were fixed and stained with filipin. MLN64-GFP is present as ring-shaped structures (*green rings* in *E*) at the surface of enlarged cholesterol-loaded lysosomes (*blue* with filipin staining in *F*). Mobile late endosomal tubules are rarely present in these cholesterol-laden cells. *A–D* were obtained with a CCD camera. *E* and *F* are confocal. *Bars*, 10 μm.

green and red signals was expected as shown in supplemental movie 4.

The MLN64 START Domain Transfers Cholesterol from Sterol-rich Donor Liposomes to Acceptor Mitochondrial Membranes and Stimulates Progestin Synthesis by Placental Mitochondria—To document that the MLN64 START domain can indeed function as a sterol transfer protein, we tested the ability of recombinant MLN64 START domain to promote the movement of [^{14}C]cholesterol from sterol-rich phosphatidylcholine unilamellar liposomes to acceptor membranes (heat-treated mitochondria) in an established assay system that is corrected for sterol transfer resulting from fusion or trapping of liposomes with acceptor membranes (14). The recombinant MLN64 START domain stimulated cholesterol transfer from liposomes in a dose- and time-dependent manner (Fig. 4). The sterol transfer activity of 1 μM recombinant MLN64 START domain was ~82% of that of 1 μM sterol carrier protein 2, a well characterized lipid transfer protein. Recombinant MLN64 START domain (1 μM) also stimulated progestin synthesis by isolated human placental mitochondria by ~2-fold after 40 min of incubation, whereas an irrelevant recombinant protein, the extra domain A of human fibronection also bearing a His_6 tag (22) had no effect on steroidogenesis.

The START Domain-deleted MLN64 (ΔSTART-MLN64) Induces Cholesterol Accumulation in Lysosomes and Inhibits Steroidogenesis Activity in Transfected Cells—Comparison of late endosomal dynamics in wild type CHO cells and COS7 cells transfected with MLN64-GFP and ΔSTART-MLN64-GFP resulted in finding the dominant negative effects caused by ΔSTART-MLN64-GFP expression. Unlike MLN64-GFP, which is present in rapidly moving late endosomal tubules (Fig. 5, *A* and *D*, and supplemental movie 1), ΔSTART-MLN64-GFP is present as immobile ring-shaped structures in the perinuclear region of WT CHO cells 48–72 h after transfection (Fig. 5, *G*

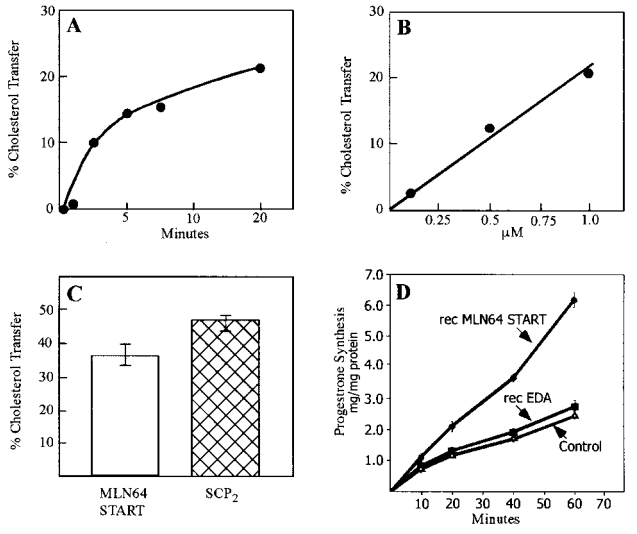

FIG. 4. **The MLN64 START domain has cholesterol transfer activity and stimulates steroid synthesis by human placental mitochondria.** *A*, time course of recombinant MLN64 START domain (1 μM) stimulated cholesterol transfer from sterol-rich liposomes to acceptor membranes. Values are means of triplicate incubations. *B*, dose response of recombinant MLN64 START domain-stimulated sterol transfer during a 20-min incubation. Values are means of triplicate incubations. *C*, comparison of the sterol transfer activity of recombinant MLN64 START domain (1 μM) and sterol carrier protein 2 (SCP_2) (1 μM) during a 20-min incubation. *D*, recombinant MLN64 START domain (1 μM) but not recombinant fibronectin extra domain A (1 μM) stimulates progesterone synthesis by isolated human placental mitochondria. Values are means ± S.D. from triplicate incubations.

and *J*, and Fig. 6, *A* and *B*). Time lapse movies of ΔSTART-MLN64-GFP-expressing living cells show no late endosomal tubular trafficking and immobile ΔSTART-MLN64-GFP containing ring-shaped compartments in the perinuclear region of the cell (supplemental movie 5). The dynamic contact and parallel alignment of mitochondria with late endosomal tubules, present in MLN64-GFP-transfected cells, were not present in cells co-transfected with ΔSTART-MLN64-GFP and StAR-RFP. The StAR-RFP enters mitochondria and labels the matrix (supplemental movie 6).

Endocytosis assays of WT CHO cells transfected with ΔSTART-MLN64-GFP revealed an alteration in the lysosomal filling of the endocytosed fluid phase marker, dextran (Fig. 5). NPC1-GFP-containing late endosomes were shown previously to load with fluorescent dextran in 2 h of uptake/chase time (5, 7). In WT CHO cells MLN64 (Fig. 5*A*) containing late endosomes loaded with dextran (Fig. 5*B*) in 2 h of uptake/chase time (Fig. 5*C*, *merged image* of Fig. 5, *A* and *B*). Co-localization of MLN64-GFP (Fig. 5*D*) and endocytosed dextran (Fig. 5*E*) is shown in 18 h of uptake/chase time (Fig. 5*F*, *merged image* of Fig. 5, *D* and *E*). In comparison, in WT CHO cells transfected with ΔSTART-MLN64-GFP and incubated with fluorescent dextran in 2 h of uptake/chase time, ΔSTART-MLN64-GFP and dextran were in separate compartments (Fig. 5*I*, *merged image* of Fig. 5, *G* and *H*). Dextran (Fig. 5*H*) was not present in the ΔSTART-MLN64-GFP-containing ring-shaped structures (Fig. 5*G*). After 18 h of uptake/chase time, dextran (Fig. 5*K*) was present only associated with ΔSTART-MLN64-GFP-containing rings (Fig. 5*F*, *merged image* of Fig. 5, *J* and *K*). This delayed dextran loading of the late endocytic compartment indicates that 1) ΔSTART-MLN64-GFP acts at the latest stage of the endocytic pathway; 2) expression of ΔSTART-MLN64-GFP shifts the late endocytic pathway from a dynamic tubular reticulum to separate and immobile compartments; and 3) the alteration of late endocytic compartments impairs the fusion capability of late endocytic compartments with earlier endocytic compartments, a phenomenon similar to a novel NPC phenotype revealed by the previous cell fusion study (7).

Because of the altered late endocytic pathway, as described above in both WT CHO cells and COS-7 cells transfected with ΔSTART-MLN64-GFP, we examined cholesterol accumulation in these cells that exhibit a phenocopy of lysosomal storage diseases. Interestingly but not surprisingly, filipin staining showed that ΔSTART-MLN64-GFP expression resulted in extensive cholesterol accumulation in the abnormally enlarged lysosomes. ΔSTART-MLN64-GFP-containing ring-shaped structures (Fig. 6, *A* and *inset*) are at the periphery of cholesterol-laden lysosomes (Fig. 6, *B* and *inset*), similar to the location of ΔSTART-MLN64 and MLN64 in transfected CT60 cells. Neither wild-type MLN64-GFP (Fig. 6*C*), START-MLN64-GFP (Fig. 6*E*), nor GFP expression (Fig. 6*G*) induced cholesterol accumulation in lysosomes (Fig. 6, *D*, *F*, and *H*). In wild-type CHO cells (as well as COS-7 cells; see below), wild-type MLN64-GFP was located in late endocytic compartments throughout the cytoplasm (Fig. 6*C*), whereas the START-MLN64-GFP (Fig. 6*E*) and GFP (Fig. 6*G*) were present in a cytoplasmic and nuclear pattern 12 h to 3 days after transfection.

As shown in Fig. 7, the dominant negative effect of ΔSTART-MLN64-GFP was also found in COS cells. COS-7 cells expressing MLN64-GFP (Fig. 7, *A*, *C*, and *D*, and supplemental movie 7) were similar to wild-type CHO cells expressing MLN64-GFP, and COS-7 cells expressing ΔSTART-MLN64-GFP (Fig. 7, *B* and *E*, and supplemental movie 8) were similar to wild-type CHO cells expressing ΔSTART-MLN64-GFP. The ΔSTART-MLN64-GFP mutant caused cholesterol accumulation in lysosomes (Fig. 7, *F* and *inset*, and supplemental movie 8) and inhibited trafficking of late endocytic tubules in COS-7 cells, whereas the START-MLN64-GFP mutant (Fig. 7*G*) was located to the nucleus and cytoplasm and did not induce cellular cholesterol accumulation in COS-7 cells.

To explore the biochemical consequences of expressing ΔSTART-MLN64-GFP, we examined the effects of co-expression of the GFP constructs on progesterone production in COS cells transfected with plasmids encoding the steroidogenic machinery. To correct for efficiency of expression of the co-transfected steroidogenic enzymes, we normalized the progesterone production by dividing it with the progesterone production of companion cells incubated in the presence of 22-OH-cholesterol, a substrate that readily enters into mitochondria. This hydroxycholesterol substrate supports maximal steroidogenic activity, limited only by the expression of the cholesterol side chain cleavage system, and thus provides an index of the transfection efficiency of the steroidogenic enzymes. We have used this normalization method routinely in our structure-function studies of the StAR protein (10, 16). Any adverse effects of the co-transfected GFP constructs on expression of the steroidogenic enzymes would be reflected in reduced conversion of 22-OH-cholesterol into progesterone. Cells transfected with the empty GFP vector produced equivalent amounts of progesterone as cells transfected with ΔSTART-MLN64-GFP (5.68 *versus* 5.99 ng/dish, respectively) (Table I). However, the COS-1 cells transfected with the empty GFP vector produced ~40% less progesterone than cells transfected with the other GFP constructs when incubated with 22-OH-cholesterol, demonstrating reduced total steroidogenic potential. The normalized progesterone production data as well as the relative steroidogenic activity (with the empty GFP vector results arbitrarily set to a value of 1.0) revealed a significant inhibitory effect of the ΔSTART-MLN64-GFP on steroidogenesis. The MLN64-GFP construct caused a modest but not significant increase in normalized progesterone production (1.3-fold above the empty

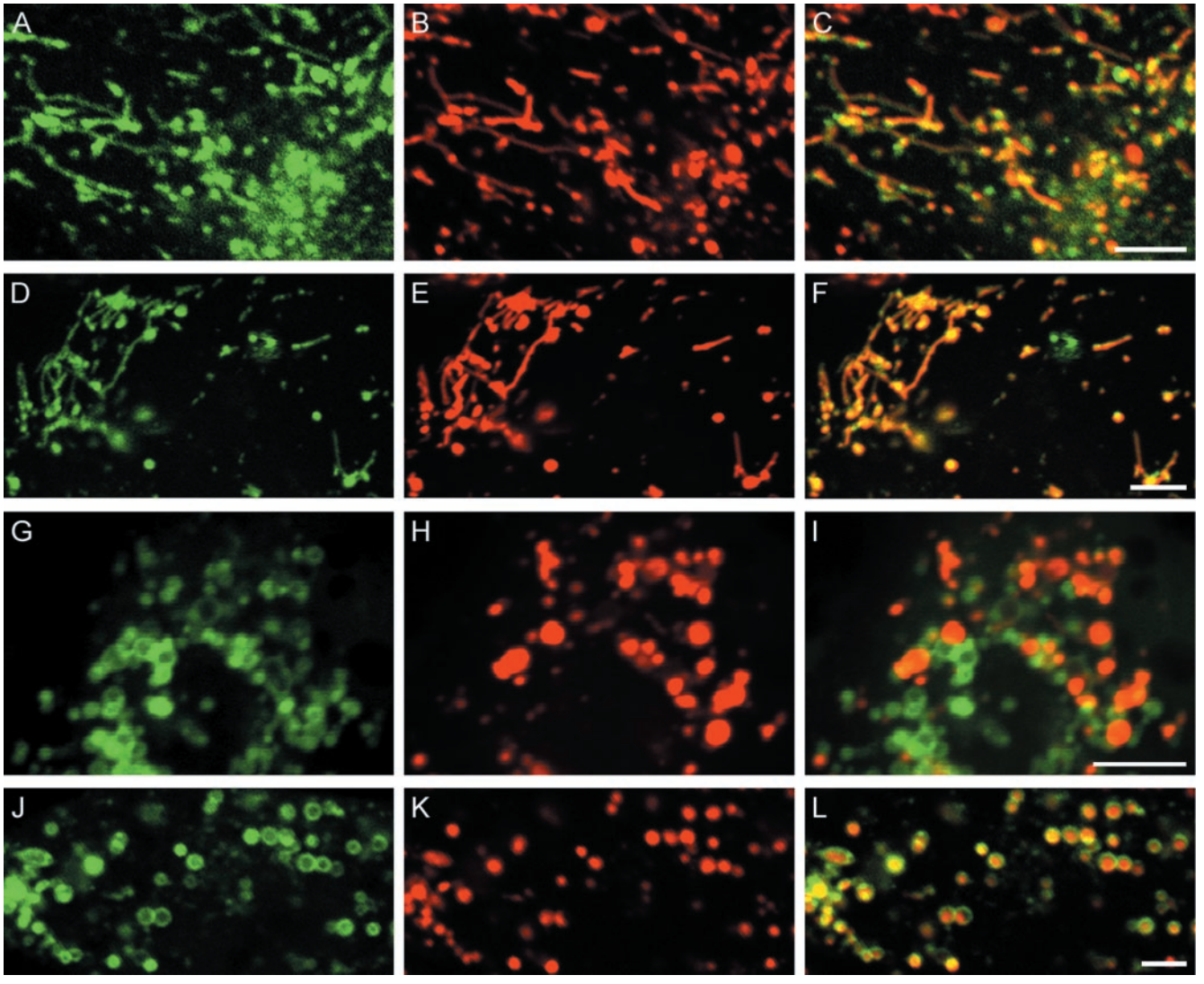

FIG. 5. **In comparison with MLN64-GFP, expression of ΔSTART-MLN64-GFP causes formation of enlarged late endocytic compartments with delayed dextran filling in wild type CHO cells.** Wild type CHO cells were transfected with MLN64-GFP (*A–F*) or ΔSTART-MLN64-GFP (*G–L*) and subsequently incubated with rhodamine-dextran in 2 h of uptake/chase time (*A–C*, *G–I*) or 18 h of uptake/chase time (*D–F*, *J–L*) and imaged at the same time 72 h after transfection. MLN64-GFP is present in tubulovesicular structures (*green*; *A* and *D*) that are filled with dextran in 2 h of uptake/chase time (*red* in *B*) and 18 h of uptake/chase time (*red* in *E*). *C* (merge of *A* and *B*) and *F* (merge of *D* and *E*) show colocalization of MLN64 and dextran. However, ΔSTART-MLN64-GFP is present in the wild type CHO cells as ring-shaped structures (*green*; *G*). Many of these ring-shaped structures do not contain core endocytosed rhodamine-dextran (*red* in *H* and *I*). After incubation of cells with dextran in 18 h of uptake/chase time, all ΔSTART-MLN64-GFP-containing compartments (*green* in *J*) are filled with dextran (*red*; *K*). A merge of *G* and *H* shows little colocalization of ΔSTART-MLN64-GFP with dextran in 18 h of uptake/chase time (*I*). A merge of *J* and *K* shows association of ΔSTART-MLN64-GFP with the surface of dextran-containing vesicles (*L*). All images were obtained from live cells with confocal double fluorescence scanning. *Bars*, 5 μm.

GFP vector), whereas the START-MLN64-GFP construct increased normalized progesterone production more than 3.7-fold, a finding consistent with our previous observations (10). The ability of the START-MLN64-GFP to increase steroid production indicates that fusion of GFP to the C terminus does not abrogate the sterol transfer activity of the START domain. To examine the effects of ΔSTART-MLN64-GFP on the utilization of LDL-derived cholesterol, we incubated transfected COS-1 cells with LDL reconstituted with [^{3}H]cholesteryl linoleate and assessed the formation of radiolabeled progesterone. The formation of radiolabeled progesterone by cells transfected with ΔSTART-MLN64-GFP (1944 ± 422 dpm/culture dish, mean ± S.D., $n = 3$) was significantly less ($p < 0.01$) than cells transfected with either the GFP empty vector (6111 ± 888 dpm/culture) or MLN64-GFP (13323 ± 2821 dpm/culture). The significantly reduced steroidogenic activity indicates that expression of ΔSTART-MLN64-GFP impairs the utilization of the lysosomal pool of cholesterol for steroidogenesis.

DISCUSSION

The present study demonstrates that 1) MLN64 resides in the NPC1-containing dynamic late endosomal reticulum; 2) overexpression of the transmembrane domain of MLN64 (ΔSTART-MLN64) induces cholesterol accumulation in lysosomes and inhibits utilization of lysosomal cholesterol by mitochondria for steroidogenesis; and 3) the START domain of MLN64 transfers cholesterol between membranes and stimulates mitochondrial steroidogenesis *in vitro*.

MLN64 Is a Component of the Dynamic Late Endosomal Tubular Reticulum, and the Dominant Negative MLN64 Mutant Causes Niemann-Pick C Phenocopy—Studies on living cells show that MLN64 is a component of a dynamic late endocytic reticulum that is composed of rapidly trafficking late endosomal tubules (5, 7). Co-localization of MLN64 and NPC1 in the dextran-labeled late endocytic tubulovesicular compartments indicates that these two membrane-spanning proteins

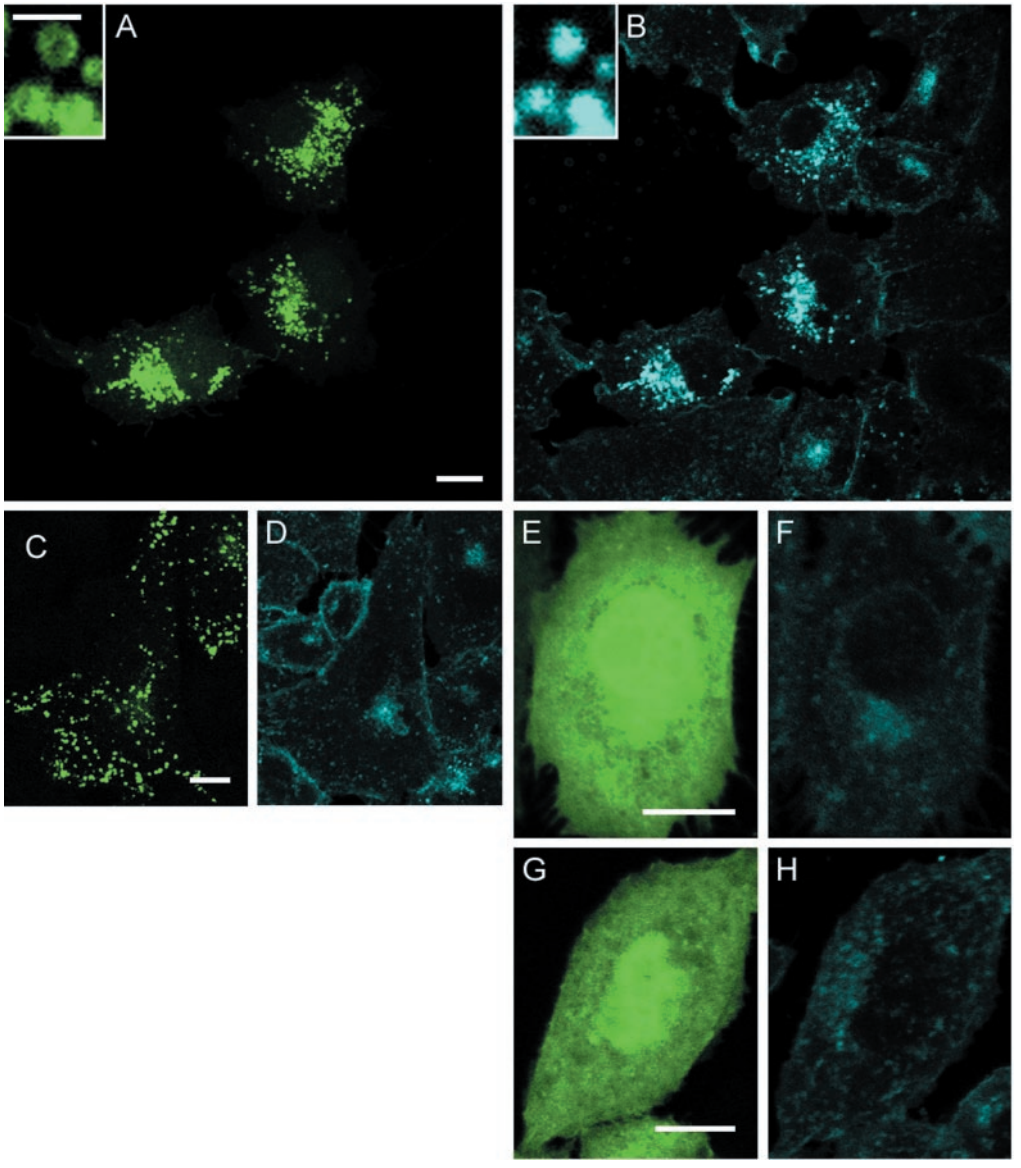

FIG. 6. **Expression of ΔSTART-MLN64-GFP causes a dominant negative effect on transfer of cholesterol out of lysosomes and inhibits late endosomal tubular trafficking in wild type CHO cells.** Shown are wild type CHO cells (*A–H*), transfected with ΔSTART-MLN64-GFP (*A* and *B*), MLN64-GFP (*C* and *D*), START-MLN64-GFP (*E* and *F*), and GFP (*G* and *H*) for 48 h and stained with filipin (*B*, *D*, *F*, and *H*). Cholesterol accumulates in ΔSTART-MLN64-GFP-expressing cells in the perinuclear region (*blue*; *B*) along with ΔSTART-MLN64-GFP (*green*; *A*). Note that as a control, the adjacent non-ΔSTART-MLN64-GFP-expressing cells do not accumulate cholesterol (*A* and *B*). Cholesterol (*inset* of *B*) accumulates in lysosomes with ΔSTART-MLN64-GFP at their peripheries (*inset* of *A*). However, wild type MLN64-GFP (*green*; *C*), START-MLN64-GFP (*green*; *E*), and GFP expression (*green*; *G*) do not induce cholesterol accumulation in lysosomes (*blue* in *D*, *F*, and *H*, respectively). MLN64-GFP is located in the late endosomal compartment (*green*; *C*), whereas the START-MLN64-GFP (*green*; *E*) and GFP (*green*; *G*) are located in the cytoplasm and nuclei. All images are confocal. A time lapse movie shows that ΔSTART-MLN64-GFP was present as ring-shaped structures in the perinuclear region of the cells but not in mobile tubules (movie 5). The movie is available as supplementary data. *Bars* for *A–H*, 10 μm; *bars* for *insets* of *A* and *B*, 2 μm.

could function in similar membrane microdomains. A previous somatic cell fusion study revealed that these late endocytic compartments normally undergo rapid content exchange, including membrane and fluid phase contents (7). MLN64 molecules may be rapidly equilibrated in the late endocytic pathway through these dynamic tubular movements that facilitate interactions between MLN64 and other components, such as NPC1 and HE1, in the late endosomal reticulum.

Visualizing the dynamics of the late endocytic pathway led to finding the dominant negative MLN64 mutant. The ΔSTART-MLN64-GFP contains all of the predicted transmembrane domains of MLN64 but lacks the START domain at the C-terminal half of the MLN64 protein. This N-terminal mutant is sufficient to mediate the biosynthetic trafficking of MLN64 from its site of synthesis, via the plasma membrane, to its final destination in the late endocytic compartment. ΔSTART-MLN64 not only follows the identical biosynthetic pathway as wild type MLN64 but also co-localizes with wild type MLN64 at the periphery of cholesterol-laden lysosomes. We had shown previously that cholesterol accumulation retards late endocytic tubular formation and mobility (7). While analyzing trafficking of MLN64 mutants, we noted that the morphology, distribution, and movement of endocytic compartments were dramatically altered in wild type CHO cells and COS-7 cells expressing ΔSTART-MLN64-GFP. In these cells, ΔSTART-MLN64-GFP containing ring-shaped structures aggregated in the perinuclear region and showed limited saltatory movement. Fluorescent filipin cytochemistry showed accumulation of cholesterol in lysosomes in ΔSTART-MLN64-GFP-transfected cells, and the mutant protein is present associated with periphery of

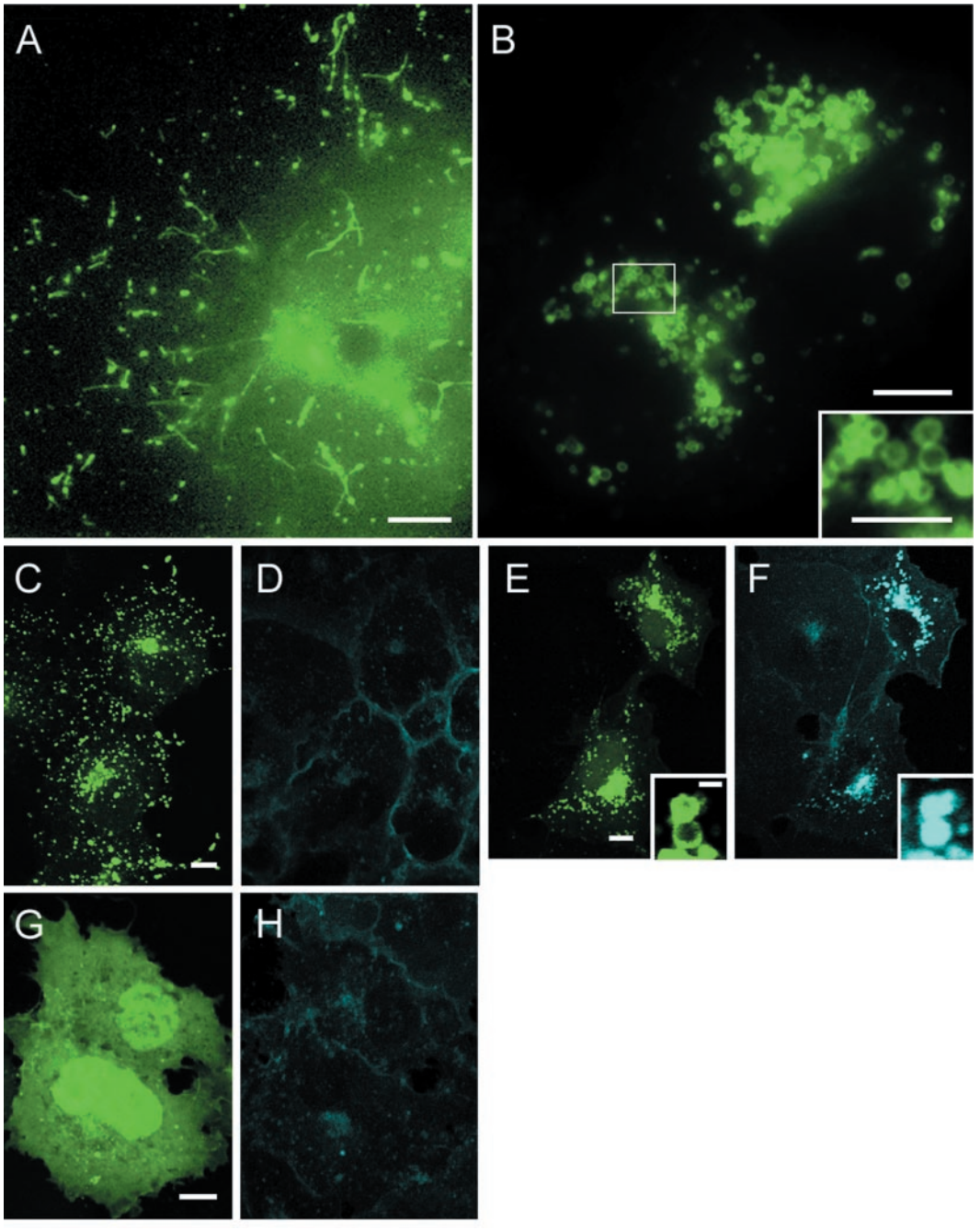

FIG. 7. **Expression of ΔSTART-MLN64-GFP causes a dominant negative effect on transfer of cholesterol out of lysosomes and inhibits late endosomal tubular trafficking in COS-7 cells.** The location of MLN64-GFP (*A* and *C*), ΔSTART-MLN64-GFP (*B* and *E*), or START-MLN64-GFP (*G*) in COS-7 cells is similar to that in wild type CHO cells. ΔSTART-MLN64-GFP expression (*green*; *E*) induces lysosomal cholesterol accumulation (*blue*; *F*) in COS-7 cells. Cholesterol is in the core of lysosomes (*inset* of *F*) with ΔSTART-MLN64-GFP at the lysosomal surface (*insets* of *E* and *B*). Adjacent non-ΔSTART-MLN64-GFP-expressing cells do not accumulate cholesterol in lysosomes (*E* and *F*). As controls, MLN64-GFP (*green*; *C*) and START-MLN64-GFP (*green*; *G*) did not induce cholesterol accumulation (*blue*; *D* and *H*) in COS-7 cells. Living COS-7 cells transfected with MLN64-GFP (*green*; *A*) and ΔSTART-MLN64-GFP (*green*; *B*) and cultured in 10% fetal bovine serum-containing medium for 72 h were imaged with a CCD camera. Cells were imaged at 20 °C to slow the movement of the late endocytic compartment. Time lapse movies show that MLN64-GFP traffics in tubules and small vesicles throughout COS-7 cells (movie 7). However, ΔSTART-MLN64-GFP was present as ring-shaped structures in the perinuclear region of the cell but not in mobile tubules (movie 8). Time lapse movies are available as supplementary data. *A* and *B* were obtained with a CCD camera. *C–H* are confocal. *Bars* for *A–H*, 10 μm; *bars* for *insets* in *B*, 5 μm; *bars* in *E* and *F*, 2 μm.

these cholesterol-laden lysosomes. This mutant MLN64-induced lysosomal cholesterol lipidosis mimics the NPC phenotype.

The finding that ΔSTART-MLN64 colocalizes with wild type MLN64 and that overexpression of ΔSTART-MLN64 results in cholesterol accumulation in lysosomes suggests that endogenous MLN64 facilitates egress of cholesterol out of these lysosomes. The ability of truncation mutants consisting of the transmembrane domains to prevent the function of endogenous wild-type proteins involved in cholesterol metabolism has also been reported in the case of sterol response element-binding protein cleavage-activating protein (23). The dominant negative effect caused by ΔSTART-MLN64 also suggests that another unknown protein may promote the function of MLN64 and that the overexpressed ΔSTART-MLN64 interacts with this component, thus blocking the endogenous MLN64 func-

TABLE I
The ΔSTART-MLN64-GFP construct inhibits steroidogenesis

COS-1 cells were transfected with plasmids expressing the human cholesterol side chain cleavage and 3β-hydroxysteroid dehydrogenase enzymes and the indicated plasmids. Cells were cultured in the absence (−) or presence (+) of (22*R*)-hydroxycholesterol (5 μg/ml). Progesterone production was determined by radioimmunoassay. Values present are means ± S.E. from eight separate experiments in which each treatment group contained triplicate cultures. Relative steroidogenic activities of the constructs are calculated normalizing progesterone production to total cholesterol side chain cleavage and 3β-hydroxysteroid dehydrogenase activity as determined in the presence of (22*R*)-hydroxycholesterol. The normalized data were expressed relative to the empty GFP vector control to determine relative activity. Normalized data were analyzed for statistical significance by Mann-Whitney U test. Values with a different superscript letter (a–c) are significantly different from all others in the column ($p < 0.02$).

Construct	Progesterone production (ng/dish)		Normalized activity	Relative activity
	−	+		
Empty GFP vector	5.68 ± 0.73	127.5 ± 22.4	0.048 ± 0.007	1[a]
MLN64-GFP	11.13 ± 1.67	200.7 ± 36.1	0.064 ± 0.012	1.30 ± 0.15[a]
START-MLN64-GFP	28.48 ± 4.4	222.7 ± 47.0	0.137 ± 0.013	3.05 ± 0.28[b]
ΔSTART-MLN64-GFP	5.99 ± 0.94	207.5 ± 32.6	0.029 ± 0.004	0.63 ± 0.09[c]

tion. The identification of the factor that interacts with MLN64 may lead to the further understanding of protein-protein interactions in the late endocytic compartments as well as cholesterol trafficking. Among the potential MLN64-interacting proteins are NPC1 and HE1, both of which are involved in cholesterol trafficking and homeostasis in the late endocytic compartment. Alternatively, MLN64 may function as a homodimer, and the truncation mutant may prevent dimerization of endogenous MLN64.

The START Domain of MLN64 Mediates Utilization of LDL-derived Lysosomal Cholesterol by Steroidogenic Mitochondria—The START domain of MLN64 shares high (35%) sequence identity within the START domain in the StAR protein, which is abundant in steroidogenic cells (24). The START domains of both MLN64 and StAR are similar in their abilities to bind cholesterol and stimulate steroidogenesis (10, 13). StAR is known to mobilize cholesterol from the cholesterol-rich outer mitochondrial membrane to the inner mitochondrial chamber, where the first step in steroidogenesis occurs, conversion of cholesterol to pregnenolone (25). In this study, biochemical analysis demonstrates that steroidogenesis by mitochondria is inhibited when blockage of cholesterol trafficking out of lysosomes by ΔSTART-MLN64 occurs. Our data also show that the START domain in MLN64 can transfer cholesterol from donor liposomes to acceptor mitochondrial membranes and stimulate progestin synthesis by placental mitochondria, suggesting that MLN64 effects cholesterol egress out of lysosomes and mediates utilization of lysosomal cholesterol by mitochondria. The ~40% inhibition of progesterone production in COS cells transfected with ΔSTART-MLN64-GFP compared with that observed with MLN64-GFP is consistent with the 50% reduction in progesterone secretion by granulosa treated with drugs that produce the Niemann-Pick type C phenotype of lysosomal cholesterol storage (25). The inhibition of utilization of LDL-derived cholesterol for steroidogenesis was, however, more profound (68% inhibition compared with empty vector-GFP and 85% inhibition compared with MLN64-GFP), indicating a key role for MLN64 in the trafficking of LDL-derived cholesterol. Collectively, these findings indicate that a portion of the steroidogenic pool of cholesterol moves through the late endosomal system prior to reaching mitochondria, where the first committed step in steroid hormone biosynthesis takes place.

The MLN64-containing compartment may deliver cholesterol substrate to mitochondria in steroidogenic cells, perhaps through transient interactions of the MLN64 START domain associated with the dynamic late endosomal compartment with the outer mitochondrial membranes. It is noticeable that both late endosomal tubular trafficking and mitochondria movement are microtubule dependent (7, 26). Using dual color time lapse imaging techniques, we found that the MLN64-GFP-containing late endosomal tubules align parallel to StAR-RFP-labeled mitochondria and transiently contact mitochondria, providing evidence for spatial interaction between two sterol-related intracellular organelles (supplemental movie 4). Because we have observed fragments of MLN64 containing the START domain in placental cell extracts (10) and also in placental mitochondrial preparations,[2] it is possible that the cleaved START domain transports cholesterol from the late endosomes/lysosomes to the mitochondria. The START domain may also promote movement of cholesterol from the outer to the inner mitochondrial membrane, where the cholesterol side chain cleavage enzyme resides. This is believed to be the process stimulated by StAR (25). However, the human placenta does not express StAR (16), and we have previously postulated that MLN64 subserves this role of StAR in the human placenta (10). The present observations are fully consistent with this notion. The fact that exogenous MLN64 START domain augments mitochondrial steroidogenesis indicates that whatever endogenous MLN64 is present in the mitochondrial preparations is not sufficient to drive maximal hormone production. This raises the possibility that regulation of MLN64 levels contributes to the control of placental steroidogenesis. Based on our observations on the effects of the ΔSTART-MLN64-GFP construct on accumulation of free cholesterol and impairment of steroidogenesis, we conclude that MLN64 is directly involved in lysosomal cholesterol mobilization. MLN64 may have an additional role in steroidogenic cells, where it mediates delivery of substrate to the mitochondrial cholesterol side chain cleavage system.

Acknowledgment—We thank Dr. T. Y. Chang for the gift of CT60 cells.

REFERENCES

1. Blanchette-Mackie, E. J. (2000) *Biochim. Biophys. Acta* **1486,** 171–183
2. Brown, M. S., and Goldstein, J. L. (1999) *Proc. Natl. Acad. Sci. U. S. A.* **96,** 11041–11048
3. Carstea, E. D., Morris, J. A., Coleman, K. G., Loftus, S. K., Zhang, D., Cummings, C., Gu, J., Rosenfeld, M. A., Pavan, W. J., Krizmanm, D. B., Nagle, J., Polymeropoulos, M. H., Sturley, S. L., Ioannou, Y. A., Higgens, M. E., Comly, M., Cooney, A., Brown, A., Kaneski, C. R., Blanchette-Mackie, E. J., Dwyer, N. K., Neufeld, E. B., Chang, T. -Y., Liscum, L., Strauss, J. F., III, Ohno, K., Zeigler, M., Garmi, R., Sokol, J., Markie, D, O'Neill, R. R., van Diggelen, O. P., Elleder, M., Patterson, M. C., Brady, R. O., Vanier, M. T., Pentchev, P. G., and Tagle, D. A. (1997) *Science* **277,** 228–231
4. Naureckiene, S., Sleat, D. E., Lackland, H., Fensom, A., Vanier, M. T., Wattiaux, R., Jadot, M., and Lobel, P. (2000) *Science* **290,** 2298–2301
5. Zhang, M., Dwyer, N. K., Neufeld, E. B., Love, D. C., Cooney, A. D., Comly, M., Patel, S., Watari, H., Strauss, J. F., III, Pentchev, P. G., Hanover, J. A., and Blanchette-Mackie, E. J. (2001) *J. Biol. Chem.* **276,** 3417–3425
6. Watari, H., Blanchette-Mackie, E. J., Dwyer, N. K., Watari, M., Neufeld, E. B., Patel, S., Pentchev, P. G., and Strauss, J. F., III (1999) *J. Biol. Chem.* **274,** 21861–21866
7. Zhang, M., Dwyer, N. K., Love, D. C., Cooney, A., Comly, M., Neufeld, E., Pentchev, P. G., Blanchette-Mackie, E. J., and Hanover, J. A. (2001) *Proc. Natl. Acad. Sci. U. S. A.* **98,** 4466–4471
8. Davies, J. P., Chen, F. W., and Ioannou, Y. A. (2000) *Science* **290,** 2295–2298

[2] F. Martinez, L. K. Christenson, and J. F. Strauss III, unpublished observations.

9. Okamura, N., Kiuchi, S., Tamba, M., Kashima, T., Hiramoto, S., Baba T., Dacheux, F., Dacheux, J. L., Sugita, Y., and Jin, Y. Z. (1999) *Biochim. Biophys. Acta.* **1438,** 377–387
10. Watari, H., Arakane, F., Moog-Lutz, C., Kallen, C. B., Tomasetto, C., Gerton, G. L., Rio, M. C., Baker, M. E., and Strauss, J. F., III (1997) *Proc. Natl. Acad. Sci. U. S. A.* **94,** 8462–8467
11. Petrescu, A. D., Gallegos, A. M., Okamura, Y., Strauss, J. F., III, and Schroeder, F. (2001) *J. Biol. Chem.* **276**, 36970–36982
12. Alpy, F., Stoeckel, M. E., Dierich, A., Escola, J. M., Wendling, C., Chenard, M. P., Vanier, M. T., Gruenberg, J., Tomasetto, C., and Rio, M. C. (2001) *J. Biol. Chem.* **276,** 4261–4269
13. Tsujishita, Y., and Hurley, J. H. (2000) *Nat. Struct. Biol.* **7,** 408–414
14. Kallen, C. B., Billheimer, J. T., Summers, S. A., Stayrook, S. E., Lewis, M., and Strauss, J. F., III (1998) *J. Biol. Chem.* **273,** 26285–26288
15. Harikrishna, J. A., Black, S. M., Szkaz, G. D., and Miller, W. L. (1993) *DNA Cell Biol.* **12,** 371–379
16. Sugawara, T., Holt, J. A., Driscoll, D. A., Strauss, J. F., III, Lin, D., Miller, W. L., Patterson, D., Clancy, K. P., Hart, I. M., Clark, B. J., and Stocco, D. M. (1995) *Proc. Natl. Acad. Sci. U. S. A.* **92,** 4778–4782
17. Krieger, M., Brown, M. S., Faust, J. R., and Goldstein, J. L. (1978) *J. Biol. Chem.* **253,** 4093–4101
18. Soto, E., Silavin, S. L., Tureck, R. W., and Strauss, J. F., III (1984) *J. Clin. Endocrinol. Metab.* **58,** 831–837
19. Martinez, F., Kiriakidou, M., and Strauss, J. F., III (1997) *Endocrinology* **138,** 2172–2183
20. Neufeld, E. B., Wastney, M., Patel, S., Suresh, S., Cooney, A. M., Dwyer, N. K., Roff, C. F., Ohno, K., Morris, J. A., Carstea, E. D., Incardona, J. P., Strauss, J. F., III, Vanier, M. T., Patterson, M. C., Brady, R. O., Pentchev, P. G., and Blanchette-Mackie, E. J. (1999) *J. Biol. Chem.* **274,** 9627–9635
21. Ko, D. C., Gordon, M. D., Jin, J. Y., and Scott, M. P. (2001) *Mol. Biol. Cell* **12,** 601–614
22. Okamura, Y., Watari, M., Jerud, E. S., Young, D. W., Ishizaka, S. T., Rose, J., Chow, J. C., and Strauss, J. F., III (2001) *J. Biol. Chem.* **276,** 10229–10233
23. Tong, Y., Goldstein, J. L., and Brown, M. S. (2000) *J. Biol. Chem.* **275,** 29881–29886
24. Christenson, L. K., and Strauss, J. F., III (2000) *Biochim. Biophys. Acta* **1529,** 175–187
25. Watari, H., Blanchette-Mackie, E. J., Dwyer, N. K., Sun, G., Glick, J. M., Patel, S., Neufeld, E. B., Pentchev, P. G., and Strauss, J. F., III (2000) *Exp. Cell Res.* **255,** 56–66
26. Yaffe, M. P. (1999) *Science* **283,** 1493–1497